Vol 18 No 5, May 2009
1674-1056/2009/18(05)/1991-05
Chinese Physics B
© 2009 Chin. Phys. Soc.
and IOP Publishing Ltd

The stabilization effect of substituted atoms and magnetism for intermetallic compounds $YFe_{12-x}Cr_x$*

Ma Huan-Feng(麻焕锋)[a], Huang Zheng(黄 整)[a)†], Chen Bo(陈 波)[b],
Qiang Wei-Rong(强伟荣)[a], and Pan Min(潘 敏)[a]

[a] *School of Physical Science and Technology, Southwest Jiaotong University, Chengdu* 610031, *China*
[b] *Institute of Nuclear Physics and Chemistry, China Academy of Engineering Physics, Mianyang* 621900, *China*

(Received 1 January 2008; revised manuscript received 4 November 2008)

Based on density functional theory, using the scheme of the linearized augmented plane wave and the improved local orbital (APW+*lo*), this paper analyses and calculates the lattice parameters, formation energy and magnetism of the rare-earth permanent magnetic materials $YFe_{12-x}Cr_x$ ($x = 0 \sim 5$). The stabilization effect and the possible positions of the substituted atom Cr are analysed. Magnetic moments for the system and the atoms are obtained.

Keywords: $YFe_{12-x}Cr_x$, density functional theory, formation energy, magnetic moment
PACC: 7128, 7520H, 7530M

1. Introduction

In searching for new materials for the fabrication of permanent magnets, different Fe-rich rare earth intermetallic compounds of the type R(Fe, M)$_{12}$ have been studied already.[1−6] The pure binary RFe_{12} compound does not exist, but de Mooij and Buschow[7] discovered that the structure can be stabilized by replacing a small fraction of Fe by the M atoms Ti, V, Cr, Mo, W, or Si. Moze and Busshow[8] analysed the magnetic structure and preferred the site occupation of Cr in the compound $YFe_{10}Cr_2$. Jaswal *et al* [9] reported the study of the electronic structure and magnetism for $YFe_{10}Cr_2$ based on the linear-muffin-tin-orbitals (LMTO) method in the semi-relativistic approximation. Coehoorn[10] presented the scalar relativistic band-structure calculation of the electronic structure and magnetism for the hypothetical YFe_{12} and YFe_8Cr_4 by using the augmented-spherical-wave (ASW) method with the local-spin-density- functional (LSDF) approximation. The structure and magnetism of $YFe_{12-x}Cr_x$ have been studied intensively, but there still exist some problems to solve: Why can pure RFe_{12} not exist? Why can the substituted chromium atoms stablilize $YFe_{12-x}Cr_x$ and the tetragonal $ThMn_{12}$ structure? And in which site can the chromium atoms replace the iron atoms?

In the present paper, the energy of $YFe_{12-x}Cr_x$ ($x = 0 \sim 5$) was calculated for the ternary Y-Fe-Cr system, using the full-potential augmented plane wave (APW) method with improved local orbitals (APW+*lo*) based on the generalized gradient approximation (GGA). Magnetic moments for the system are calculated. The stabilization effect and the sites of the substituted chromium atoms are discussed.

2. Method

The linearized APW (LAPW) method is among the most accurate methods of performing electronic structure calculations for crystals. It is based on density functional theory (DFT) for the treatment of exchange and correlation and uses e.g. GGA. Like most energy-band methods, the LAPW method is a procedure for solving the Kohn–Sham equations for the ground state density, total energy, and eigenvalues (energy bands). In the procedure, every unit cell volume is partitioned into two regions: non-overlapping muffin-tin spheres around each atom and the remaining interstitial area. Two different sets of basis functions are used in the two regions. For wavefunctions inside the atomic sphere a linear combination of ra-

*Project supported by the Science and Technology Foundation of China Academy of Engineering Physics (Grant No 20050212).
†E-mail: zhhuang@home.swjtu.edu.cn

dial functions time spherical harmonics, and in the interstitial region a plane wave expansion is used. In order to increase the flexibility of the basis and to make possible a consistent treatment of semi-core and valence states in one energy window, additional basis functions (local orbitals, LO) are added. Sjöstedt, Nordstrom, and Singh[11] have shown that the standard LAPW method with the additional constraint on the plane waves of matching in value and slope to the solution inside the sphere is not the most efficient way. They suggested a new scheme with improved local orbitals (denoted as *lo* to distinguish from the standard LO), which does not require the wavefunctions to be smooth at the sphere boundary. Madsen *et al*[12] showed that the new scheme (denoted as APW+*lo*) converges practically to identical results to the standard LAPW, but leads to significantly smaller basis sets and less computational time.

In the present paper, the calculations were performed within the framework of DFT implemented in the WIEN2K code,[13] using the APW+*lo* scheme with the exchange-correlation potential based on the Perdew, Burke, and Ernzerhof formalism of GGA. The energy cutoff for the plane wave expansion of the wavefunction in the interstitial region was chosen to be –6.0 Ryd. A muffin-tin radius of 2.7 a.u. for the Y atoms and 2.1 a.u. for Fe and Cr was used, a mesh of 112 k points was generated in the irreducible wedge of the Brillouin zone and the energy convergence was selected to be 0.0001 Ryd, validating that the added k-points will not change the energy convergence.

3. Results and discussion

3.1. Crystal structure

The crystal structures and energies of Y, Fe, Cr, and $YFe_{12-x}Cr_x$ ($x = 0 \sim 5$) are optimized and calculated. $YFe_{12-x}Cr_x$ ($x = 0 \sim 5$) intermetallic compounds crystallize in the body-centred-tetragonal $ThMn_{12}$-structure with space group $I4/mmm$,[8,12] including one site, $2a$, for Y atoms, and three sites, $8f$, $8i$, and $8j$ for Fe or Cr atoms, shown in Fig. 1. The metallic Fe and Cr crystallize in a body-centred-cubic structure with space group $Im-3m$,[14], Y in a hexagonal structure with space group $P63/mmc$.[14]

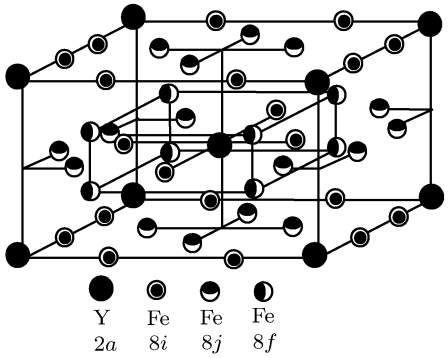


Fig.1. Crystallographic structure of YFe_{12}.[5]

The lattice constants and calculated energies are listed in Table 1. The lattice constants of calculation for all the metals and the intermetallic compounds are smaller than those of experiment, except for the element yttrium.

Table 1. Lattice constants and energies.

	this work				exp.		
	space group	a/nm	c/nm	E/Ryd	a/nm	c/nm	Ref.
Y	$P63/mmc$	0.3595	0.5871	–6771.4246	0.3551	0.5799	[14]
Fe	$Im-3m$	0.2829	0.2829	–2545.5848	0.2866	0.2866	[14]
Cr	$Im-3m$	0.2866	0.2866	–2101.7552	0.2885	0.2885	[14]
YFe_{12}	$I4/mmm$	0.8338	0.4707	–37318.5142			
$YFe_{11}Cr$	$Imm2$	0.8388	0.4711	–36874.7094	0.8460	0.4753	[10]*
$YFe_{10}Cr_2$	$P4/mmm$	0.8372	0.4702	–36430.8839	0.8463	0.4755	[7]
YFe_9Cr_3	$Imm2$	0.8303	0.4663	–35987.0461	0.8450	0.4748	[10]*
YFe_8Cr_4	$I4/mmm$	0.8301	0.4662	–35543.2226	0.8445	0.4745	[10]*
YFe_7Cr_5	$Imm2$	0.8301	0.4662	–35099.3769			

*The experimental lattice constants of $YFe_{11}Cr$, YFe_9Cr_3 and YFe_8Cr_4 are estimated by extrapolation from the data in Ref. [10].

It can be seen that the calculated lattice constants of $YFe_{12-x}Cr_x$ generally decrease with the concentration of chromium ($x = 1 \sim 5$). Some experiments show[1,15–18] that the unit-cell volume increase with x ($x = 0 \sim 4$)

for $YFe_{12-x}M_x$ as M=Ti, V, Mo, and W, but decreases as M=Cr. The variation of the lattice constants listed in Table 1 represents the experimental results as $x = 1 \sim 5$, but the lattice constants of YFe_{12} are smaller than those of $YFe_{11}Cr$ by 1%. The chromium atom would expand the lattice volume of $YFe_{11}Cr$, because the atomic volume of chromium is larger than that of iron. However, the lattice volume would decrease as more chromium atoms substitute for the iron atoms at the $8i$ site, because the half-full occupied orbitals 4s and 3d by the configuration $4s^13d^5$ of the chromium favour the formation of bonds with the fully occupied configuration $4s^23d^{10}$ by the partnership of electrons.

Table 2 lists the parameters of the atomic sites for $YFe_{12-x}Cr_x$.[8] It is shown that there should be three available sites for the iron element in YFe_{12} with the $ThMn_{12}$-structure, $8i$, $8j$,and $8f$, each of them including four equivalent iron atoms.

Table 2. Parameters of the atomic sites for $YFe_{12-x}Cr_x$.

atom	Y	Fe, Cr		
	$2a$	$8i$	$8j$	$8f$
site	(0.0, 0.0, 0.0)	(0.3594, 0.0, 0.0)	(0.0, 0.2234, 0.5)	(0.25, 0.25, 0.25)
		(0.6406, 0.0, 0.0)	(0.0, 0.7766,0.5)	(0.25, 0.75, 0.25)
		(0.0, 0.3594, 0.0)	(0.2234, 0.0, 0.5)	(0.25, 0.25, 0.25)
		(0.0, 0.6406, 0.0)	(0.7766, 0.0, 0.5)	(0.75, 0.75, 0.25)

Table 3 lists the calculated energies of $YFe_{11}Cr$ for the chromium atom substituting for the iron atom at the different sites, showing that the chromium atom should replace one of the iron atoms at site $8i$ because of the lowest energy. For a similar reason, all the chromium atoms should also replace the iron atoms at site $8i$ for $YFe_{10}Cr_2$, YFe_9Cr_3, and YFe_8Cr_4, and a redundant chromium atom would occupy the $8j$ site for YFe_7Cr_5. This agrees with the experimental fact observed by neutron diffraction for $YFe_{12-x}Cr_x$.[8]

Table 3. Energy of $YFe_{11}Cr$ for the Cr atom at different sites.

site	$8f$	$8j$	$8i$
E/Ryd	–36874.6966	–36874.6956	–36874.7094

3.2. Stabilization

The energy for the formation reactions $kY + mFe + nCr \rightarrow Y_kFe_mCr_n$ can be estimated as $\Delta E_f = E(Y_kFe_mCr_n) - kE(Y) - mE(Fe) - nE(Cr)$. All the calculated formation energies (ΔE_f) of $YFe_{12-x}Cr_x$ ($x = 0 \sim 5$) are listed in Table 4.

Table 4. Formation energy of $YFe_{12-x}Cr_x$, and Y_2Fe_{17} (Ryd/f.u.).

	YFe_{12}	$YFe_{11}Cr$	$YFe_{10}Cr_2$	YFe_9Cr_3	YFe_8Cr_4	YFe_7Cr_5
E_f	–0.0720	–0.0968	–0.1009	–0.0927	–0.0988	–0.0827

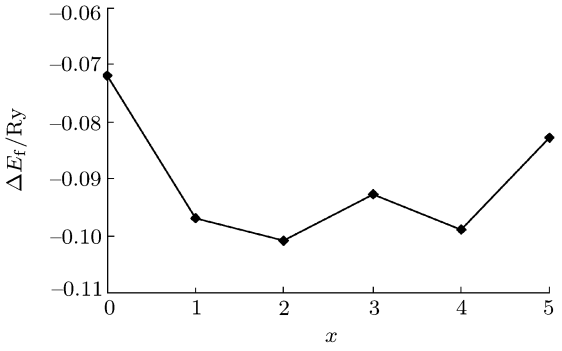


Fig.2. Relationship of the formation energy to the composition of $YFe_{12-x}Cr_x$.

Figure 2 shows that the calculated formation energies of $YFe_{12-x}Cr_x$ ($x = 1 \sim 4$) are obviously lower than those of YFe_{12} and YFe_7Cr_5; this implies that the structure can be stablized by replacing the iron atoms at the $8i$ site by Cr atoms ($x = 1 \sim 4$). This agrees with the experimental results of x-ray examination obtained by Buschow.[18]

3.3. Magnetic properties

Table 5 gives the calculated total and local magnetic moments of $YFe_{12-x}Cr_x$ ($x = 0 \sim 4$). Here the calculated magnetic moment of $YFe_{10}Cr_2$ ($15.53\mu_B$) is comparable with the experimental result ($14.5\mu_B$)

of neutron powder diffraction at 295 K by Moze and Buschow.[7] The calculated total and local magnetic moments of YFe_{12} and YFe_8Cr_4 in this work are comparable with the results calculated by Coehoorn[10] using the ASW method, and those of $YFe_{10}Cr_2$ with the results by Jaswal *et al*[9] using the LMTO method. The total magnetic moments of $YFe_{12-x}Cr_x$ and the local moments of Fe atoms in Table 5 all decrease with substitution of chromium. Generally, the sequence of the moments of Fe atoms at the different sites in $YFe_{12-x}Cr_x$ in Table 5 is $8i > 8j > 8f$, and their values split with the addition of chromium atoms because of the symmetry break. For example, $YFe_{11}Cr$ has one iron atom (singlet) with moment $2.47\mu_B$ at the $8i$ site, two equivalent iron atoms (doublet) with moment $2.40\mu_B$, and a chromium atom with moment $-1.97\mu_B$. The four iron atoms at the $8j$ site of $YFe_{11}Cr$ split with three moment values, $2.27\mu_B$ (singlet), $2.18\mu_B$ (singlet) and $2.10\mu_B$ (doublet). The four iron atoms at the $8f$ site of $YFe_{11}Cr$ remain equivalent (quartet) with moment $1.86\mu_B$. The calculated spin-polarized densities of states (DOS) are shown in Fig. 3. Here Figs. 3(a) and 3(c) are the total DOS of YFe_{12} and YFe_9Cr_3, and Figs. 3(b) and 3(d) are the local DOS of the Fe atom at the $8i$ site, respectively. It is obvious that all the peaks of the total and local DOS of spin-up for YFe_{12} appear under the Fermi level (E_F), and the values of DOS over E_F are very small. At both sides of the Fermi level, there are peaks of the spin-down DOS for YFe_{12}. The total and local spin-up DOS over the Fermi level would increase obviously with the substitution of chromium atoms, but the distributions of the total and local spin-down DOS hardly change. The local DOS distribution of the $8j$ and $8f$ sites have the similar characteristics as that of $8i$. This indicates that the chromium plays the role of not only diluting the Fe concentration, but also decreasing the moments of the iron.

Table 5. Local and total magnetic moments (μ_B/f.u.).

	YFe_{12}	$YFe_{11}Cr$	$YFe_{10}Cr_2$	YFe_9Cr_3	YFe_8Cr_4
Y($2a$)	–0.24 (–0.39)[a]	–0.25	–0.22 (–0.33)[b]	–0.17	–0.12 (–0.22)[a]
Fe($8i$)	2.51^{q} (2.32)[a]	2.47^{s} 2.40^{d}	2.14^{d} (2.23)[b]	2.28^{q}	
Cr($8i$)		-1.97^{s}	-1.22^{d} (–1.18)[b]	-1.67^{d} -1.61^{d}	-0.44^{q} (–0.66)[a]
Fe($8j$)	2.24^{q} (2.26)[a]	2.27^{s} 2.18^{s} 2.10^{d}	2.15^{d} 1.86^{d} (2.08)[b]	2.03^{s} 1.92^{s} 1.81^{d}	1.62^{q} (1.67)[a]
Fe($8f$)	1.87^{q} (1.86)[a]	1.86^{q}	1.62^{d} 1.61^{d} (1.77)[b]	1.66^{q}	1.36^{q} (1.41)[a]
total	25.43 (24.2)[a]	20.24	15.53 (17.2)[b]	12.07	9.71 (8.8)[a]

s: singlet, d: doublet, q: quartet. a: Ref.[10], b: Ref.[9].

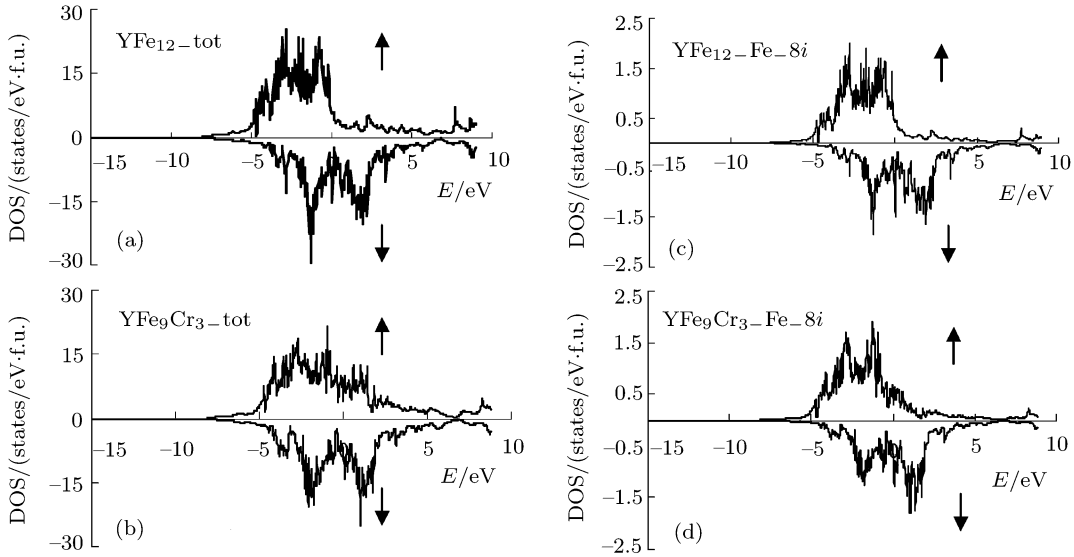


Fig.3. The total and local spin-polarized densities of states of YFe_{12} andYFe_9Cr_3. The zero on the energy axis corresponds to the Fermi energy. Here f.u. denotes formula unit.

4. Conclusions

Based on DFT, using full-potential LAPW and improved local orbitals, the structures, formation energies and magnetism of the ternary metallic compounds $YFe_{12-x}Cr_x$ are optimized and calculated. The energies of YFe_{12} and YFe_7Cr_5 are higher than those of $YFe_{12-x}Cr_x$ ($x = 1 \sim 4$), which explains the stabilization of the chromium atoms substuting the iron atoms in the compound $YFe_{12-x}Cr_x$ with $ThMn_{12}$ structure, and a chromium concentration of less than $x = 4$. Energy analysis confirms a strong site preference of Cr for the $8i$ site. The calculated magnetic moments of $YFe_{12-x}Cr_x$ are accepted by comparison with the experimental results, and analysed with the local and total DOS.

References

[1] Han X F, Yang F M, Zhu J J, Pan H G, Wang Y G, Wang J L and Tang N 1997 *J. Appl. Phys.* **81** 3248

[2] Su G, Yan Y, Xu S W, Du X B, Jin H M and Wang X Q 2005 *Chin. Phys.* **14** 10

[3] Sun G A, Chen B and Du H L 2005 *Acta Phys. Sin.* **54** 9 (in Chinese)

[4] Wang W Q, Yan Y, Wang X F, Su F, Wang X Q and Jin H M 2003 *Acta Phys. Sin.* **52** 1 (in Chinese)

[5] Gao G Q, Chen B, Huang Z, Zhang X L, Sun G A, Huang H S and Yu C 2006 *Acta Phys. Sin.* **55** 6036 (in Chinese)

[6] Jiang L X, Meng J B, Xia Z Y, Chen Z J, Luo J L and Wang N L 2004 *Chin. Phys.* **13** 2131

[7] de Mooij D B and Buschow K H J 1988 *J. Less-Common Met.* **136** 207

[8] Moze O and Buschow K H J 1996 *J. Alloy Compound* **233** 165

[9] Jaswal S S, Ren Y G and Sellmyer D J 1990 *J. Appl. Phys.* **67** 4564

[10] Coehoorn R 1990 *Phys. Rev.* B **41** 11790

[11] Sjöstedt, Nordstrom L and Singh D J 2000 *Solid State Commun.* **114** 15

[12] Madsen G K H, Blaba P, Karlheinz Schwarz, Sjöstedt and Nordström L 2001 *Phys. Rev.* B **64** 195134

[13] Blaha P, Schwarz K, Madsen G K H, Kvasnicka D and Luitz J 2001 *WIEN2k, An Augmented Plane Wave +Local Orbital Program for Calculating Crystal Properties* (Techn University Wien, Austria: Institut für Physikalische and Theoretishce Chemie) ISBN 3-9501031-1-2

[14] Lide D R 1992-1993 *CRC Handbook of Chemistry and Physics* 73rd ed (Boca Raton, Florida: CRC Press)

[15] Helmhodt R B, Vleggaar J J and Buschow K H J 1988 *J. Less-Common Met.* **138** L11

[16] Moze O, Paeeti L, Solzi M and David W I F 1988 *Solid State-Commun.* **66** 465

[17] Yang Y C, Kebe B, James W J, Deportes J and Yelon W 1981 *J. Appl. Phys.* **52** 2077

[18] Buschow K H J 1988 *J. Appl. Phys.* **63** 3130